Turkish Online Journal of Qualitative Inquiry (TOJQI)
Volume 12, Issue 8, July 2021: 4124 - 4140

# Design Implementation and Assessment of Efficient Brain Tumor Detection and Classification System Using Improved Machine Learning Techniques

Nidhi Mittall[a], YashikaSaini[b],Manish Kumar Mukhija[c], Satish Kumar Alaria[d]

[a]M.Tech. Scholar, Department of Computer Science &Engineering, AIET, Jaipur, India
[b]Associate Professor, Department of Computer Science & Engineering, AIET, Jaipur, India
[c,d]Assistant Professor, Department of Computer Science & Engineering, AIET, Jaipur, India

## ABSTRACT

A tumor is a mass of tissue formed by the accumulation of abnormal cells that continue to grow. The brain is the most important organ in the human body, responsible for controlling and regulating all critical life functions for the body, and a tumor is a mass of tissue formed by the accumulation of abnormal cells that continue to grow. A brain tumor is a tumor that has grown in the brain or has spread across the brain. To yet, no one reason has been found for the development of brain tumor. Though brain tumor are uncommon (approximately 1.8 percent of all recorded cancers in the world), the death rate of malignant brain tumor is quite high due to the tumor's location in the body's most vital organ. As a result, it is critical to accurately detect brain tumor at an early stage in order to reduce mortality. As a result, we've presented a computer-assisted radiology system that will assess brain cancers from MRI scans for brain tumor diagnosis treatment. In this paper, we developed a model that accurately separates and extracts characteristics from images using the DWT and PCA techniques, as well as SVM. For medical analysis and interpretation, automated and reliable classification of MR brain images is critical. Several techniques have previously been proposed in the recent decade. We introduced a novel method for classifying a given MR brain image as normal or abnormal in this paper. The proposed approach used wavelet transform to extract features from images, then PCA to minimize the dimensionality of the features. A kernel support vector machine was used to process the reduced features (KSVM). To improve KSVM generalization, the K-fold cross validation approach was applied. The accuracy of the LIN, HPOL, and IPOL kernels is higher. We also compared our technique to previous literatures, and the results revealed that our DWT+PCA+KSVM with specific kernel method still produced the most accurate classification results.

***Keywords-*** Brain Tumor, CNN, SVM, DWT, PCA, KSVM

## 1. INTRODUCTION

Magnetic Resonance Imaging (MRI) is used in radiology to investigate the operations of human bodies and the behaviour of organisms. The magnetic field and radio waves can be used to frame these frames. It is typically used in hospitals to diagnose and resolve the infection without the use of ionising radiation for clinical research. There are a broad variety of uses of clinical findings and over

25,000 scanners are to be used worldwide. It affects the inference and processing of various claims to renown, although the impact on better outcomes of human life is doubtful. MRI is better than CT, as ionising radiation is not used as either approach could generate similar results. The steady increase in MRI demand in the social insurance industry has raised questions about price adequacy and identification. Dividing an image is an attempt to collect comparative hues or picture components into a category or class. It can be done by bundling which adds the number of colours or components to a certain category depending on the proximity of the picture's shading power and dark power.

## 2. OBJECTIVE

The main purpose of bunching a photo is to remove nuances from the photographs. The separation of images may be important to enhance by removing data from images, such as the surface, shadow, form and structure. The division was used in many areas in the sense of data extraction, such as enhanced photography, strain, rehabilitation system, i.e., web crawlers, object discovery and preparation for the clinical image. Different methods have been developed for the image division in previous decades. Fuzzy c-implies (FCM) is a remarkable technique and popular plan of grouping which divides the picture into sections depending on the contribution. After FCM, the computational unpredictability of FCM has been decreased by measuring the K-subjects. K-implies are used in a variety of applications because of their ability to package enormous knowledge rapidly. The gradable grouping is commonly used for picture division after many years. Then, with its variance Expectative Maximization, the Gaussian Mixture Model was used to cut pictures.

The goals of the study are:

a) Simulating image processing process.
b) To simulate MRI images for brain tumor analysis for feature extraction.
c) To design and simulate efficient preprocessing and classification system.
d) Application of kernel based support vector machine for the classification process.
e) Design of efficient machine learning methodology for fast and efficient segmentation of brain tumors from MRI images.

Comparative assessment of developed algorithm for performance assessment and accuracy analysis.

## 3. LITERATURE REVIEW

**Bhandari et-al [2020]**Quantitative image analysis has spawned new fields such as radiomics, which have been used to predict therapeutic outcomes. Brain tumors, particularly glioblastoma multiform, are an increasing topic of research interest (GBM). Tumor segmentation is a crucial phase in the pathology's analysis. Manual segmentation is often inconclusive since it differs from observer to observer. To address this problem, automated segmentation has been proposed. The literature has been interested in methodologies such as convolutional neural networks (CNNs), which are machine learning pipelines modeled on the biological process of neurons (called nodes) and synapses (connections). We examine into the role of CNNs in segmenting brain tumors by first learning about them and then conducting a literature search to find an example segmentation process. The future usage of CNNs is then investigated by looking into a new subject called radioomics. This research looks at quantitative aspects of brain tumors such shape, texture, and signal strength in order to predict clinical outcomes like survival and treatment response[36]

**Jin KH et-al. (2017)**present a deep convolutional neural network (CNN)-based technique for addressing ill-posed inverse problems in this research. In the last few decades, regularized iterative algorithms have become the conventional technique to ill-posed inverse problems. These approaches generate good results, but they can be difficult to implement in reality due to considerations such as the forward and adjoint operators' high computing costs and the complexity of hyperparameter selection. The discovery that unrolled iterative approaches take the form of a CNN (filtering followed by pointwise nonlinearity) when the forward model's normal operator (H*H, where H* is the adjoint of the forward imaging operator, H) is a convolution is the starting point for this research. We propose utilizing direct inversion followed by a CNN to tackle normal-convolutional inverse problems based on this observation. The direct inversion contains the system's physical model, but when the problem is ill-posed, it produces artifacts; the CNN uses a combination of multiresolution decomposition and residual learning to learn to remove these artifacts while keeping picture structure. On parallel beam X-ray computed tomography, we demonstrate the performance of the proposed network in sparse-view reconstruction (down to 50 views) in synthetic phantoms as well as real experimental sinograms. For the more realistic phantoms, the suggested network beats total variation-regularized iterative reconstruction, and reconstructing a 512 x 512 picture on the GPU takes less than a second.[37]

**Yamashita R et-al. (2018)** Convolutional neural networks (CNNs), a type of artificial neural network that has been popular in computer vision, are gaining popularity in a variety of fields, including radiology. CNN uses several building blocks like as convolution layers, pooling layers, and fully connected layers to learn spatial hierarchies of information automatically and adaptively through backpropagation. This review article addresses the fundamental concepts of CNN and how they are used to various radiological tasks, as well as the obstacles and future directions in the field of radiology. This article will also explore two obstacles in applying CNN to radiological tasks: short datasets and overfitting, as well as ways to mitigate them. Understanding the concepts, benefits, and limitations of CNN is critical for maximizing its potential in diagnostic radiology, with the objective of increasing radiologists' performance and patient care [38].

**Palash Ghosal et-al. [2019]** spoken about The brain tumour was by as one of the major and most alarming causes of death with a strong financial impact in both Western and Eastern nations. In order to help radiologists keep them from dangerous histological biopsies, differential finding and grouping (Gliomas, Meningioma and Pituitary Tumours) in MRI information are needed. In the meantime, it is also an attempt to improve the precision and safety of analyses. For this reason , various solutions have so far been suggested. At the moment, a programmed brain tumour order tool is added from the MRI information where the image cut examples are transferred to the Convolutional Neural Network (CNN)-dependent Squeeze and Excitation ResNet model. The study evaluation indicates, without knowledge improved, that the proposed CNN is 89.93% accurate in general. The increase in Knowledge expansion further increased the accuracy of glioma, meningioma, and pituitary tumours to 98.67 percent, 91.81 percent and 91.03 percent with a general accuracy of 93.83 percent separately. Promising changes in terms of impacts and characteristics were contrasted, as well as a portion of cutting-edge technology. [12]

**Navneet Agrawal et-al. [2018]** proposed a programmed system to discern tumours and edoema-separating tumour can successfully support the development and precareful evaluation of the neurosurgeon has. We then developed productive calculations that predict early biomarkers and integrate brain infection. We co-ordinated flexible solo mapping (AMSOM) with FK media for enhanced knowledge reduction through expert bunching of tissues. We also stressed the extraction of tissue. We have measured using constant clinical knowledge and reshaped it to a scale of 256x256 pixels. The image exam reveals discriptive brain designs relevant to the location of the brain tumour, which increase the mean square blackout of 14%, 12% and the accuracy of 6%. The proposed technological implementation here gives the MRI 1.5 Tesla T1 pictures with 22 highlights improved recognition and assessment yielding promising results. In this way, they are used in the brain maturity and disease study by radiologists.[13]

## 4. PROPOSED WORK

Various algorithms like c means clustering, hybrid fuzzy k-means (FKM) in short. Next, medium filter preprocessing has been performed to eliminate the sound from digital images and enhance the image quality. Then the initial stage output is given to the k-mean classification, which provides a segmented image output. Now the k-means segmented output will be clustered in order to boost the segmentation accuracy and accurate tumor detection of MR brain images. Binarization is often used to measure the tumor's size based on typography and digital imagery.

There are a number of different segmentation techniques that are described elsewhere. The following are some notable segmentation models:

- Thresholding method—voxels exceeding a certain threshold are classified as belonging to the tumor, as the name implies.
- Edge-based method: tumor borders are defined by variations in intensity between voxel edges.
- Region-growing method: a seed voxel is entered into the segmentation; similar voxels are recognized as belonging to the tumor based on this seed.
- Watershed algorithm—this is a one-of-a-kind segmentation approach in which the voxel intensities or gradients are represented by a topographical map akin to those used in geography. A boundary is assigned based on the map's'steepness.'
- Atlas method: a tumor-free guide To segment the MRI including the tumor volume, an MRI is used. The convolutional neural network has the advantage of providing the highest level of segmentation accuracy. This, however, comes at the cost of increased computational effort. Convolutional neural networks and the refining of anatomical segmentation of brain tumors can both benefit from advances in computation.

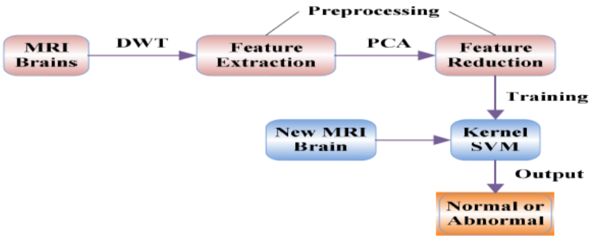

Figure 4.1 Overview of Proposed Methodology

In the discipline of machine learning, the invention of the support vector machine (SVM) was a watershed moment. High accuracy, beautiful mathematical tractability, and straightforward geometric interpretation are all advantages of SVMs. Multiple enhanced SVMs have recently increased in popularity, with kernel SVMs being the most popular and effective. The following are some of the benefits of kernel SVMs:

(1) Perform admirably in practice, with notable results in disciplines as diverse as natural language categorization, bioinformatics, and computer vision.

(2) Have a limited number of configurable parameters.

(3) Convex quadratic optimization is frequently used in training.

As a result, solutions are global and usually one-of-a-kind, avoiding the local minima that other statistical learning systems, such as neural networks, exhibit. Assume that some data points are assigned to one of two classes, and that the purpose is to determine which class a new data point will be assigned to. A data point is represented here as a p-dimensional vector, and our goal is to generate a (p1)-dimensional hyper plane. There are numerous hyper planes that could successfully classify the data. Because we can expect better behavior in response to unseen data during training, i.e., higher generalization performance, one reasonable candidate for the optimum hyper plane is the one that indicates the widest separation, or margin, between the two classes. As a result, we select the hyper plane so that the distance between it and the nearest data point on each side is as short as possible. The geometric interpolation of linear SVMs is shown in Figure 4.3, where H1, H2, and H3 are three hyper planes that can successfully classify the two classes; however, H2 and H3 do not have the highest margin, so they will not perform well with new test data. The H1 is chosen as the best classification hyper plane because it has the greatest margin to the support vectors (S11, S12, S13, S21, S22, and S23). Table 4.1 lists the formulas and parameters for three common Kernels (HPOL, IPOL, and GRB).

**Table 4.1Kernel: HPOL, IPOL & GRB**

| Name | Formula | Parameter |
|---|---|---|
| Homogeneous Polynomial (HPOL) | $k(x_i, x_j) = (x_i \cdot x_j)^d$ | $d$ |
| Inhomogeneous Polynomial (IPOL) | $k(x_1, x_j) = (x_i \cdot x_j + 1)^d$ | $d$ |
| Gaussian Radial Basis (GRB) | $k(x_i, x_j) = \exp\left(-\gamma \| \; {}_1 - x_j \|^2\right)$ | $\gamma$ |

The rationale for this stems from the fact that a square root calculation is needed. The solution will not change after it is replaced with a formula, but the problem will be transformed into a quadratic programming optimization that is simple to solve using Lagrange multipliers and normal quadratic programming techniques and programs. Traditional SMVs use a hyper plane to classify data, therefore they can't handle classification problems where different categories of data are on opposite sides of a hyper surface. To solve this problem, the kernel strategy is used on SVMs.

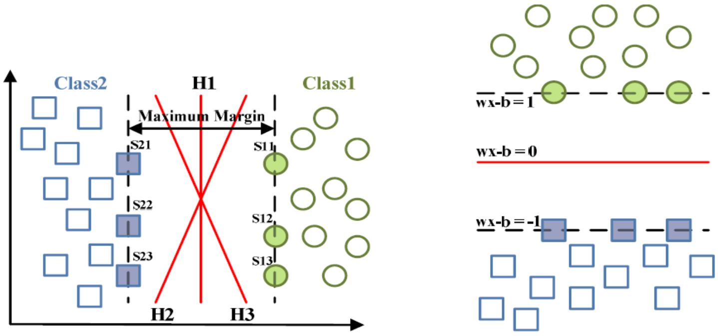

**Figure 4.2 Processing in support vector machine**

Except that every dot product is substituted by a nonlinear kernel function, the resulting algorithm is formally equivalent. The equation transformed feature space connects the kernel to the transform $\varphi(x_i)$. Although the classifier is a hyper plane in the higher-dimensional feature space, it may be nonlinear in the original input space due to the nonlinear transformation and higher dimensional transformed space.

## 5.RESULT

In this research, we suggested a new MRI brainer for the identification of the tumor, and a more detailed and time-consuming discovery of the location of the tumor. This is explores a new deep convolutional neural network algorithm to minimize the calculation time and binarization process in terms of a zone centred on the form and digital image units. After we located the tumor region and measured the CPU calculation time, we compared the outcome of the simulation with the current algorithms with the proposed shaft algorithm. Eventually, with decreased calculation time the algorithm proposed has been much better than the current algorithms.

### *5.1 Description of Database*

T2-weighted MR brain images in the axial plane with 256256 in-plane resolution were obtained from the Harvard Medical School website (URL: http://med.harvard.edu/AANLIB/), the OASIS dataset (URL: http://www.oasis-brains.org/), and the ADNI dataset (URL: http://adni.loni.ucla.edu/). We chose the T2 model because, as compared to the T1 and PET modalities, T2 images have a higher contrast and crisper vision.

Glioma, meningioma, Alzheimer's disease, Alzheimer's disease + visual agnosia, Pick's disease, sarcoma, and Huntington's disease are among the disorders represented in the dataset's aberrant brain MR images.

For each type of brain, we chose 20 photos at random. Because the dataset contains one type of normal brain and seven types of abnormal brain, 160 images were chosen, with 20 normal brain images and 140 (=7 types of diseases x 20 photos/diseases) abnormal brain images.

### *5.2 Feature Reduction*

Wavelet decomposition at three levels considerably reduces the size of the input image. The approximation coefficients of level-3, whose size is just 3232=1024, are shown in the top left corner of the wavelet coefficients image.

The number of retrieved characteristics was lowered from 65536 to 1024, as previously indicated. It is, however, still too vast to calculate. As a result, PCA is utilized to further minimize the dimensionality of features.

The variances are plotted against the number of main components, which ranges from 1 to 20. Only 19 principle components, or 1.86 percent of the original characteristics, were shown to be capable of preserving 95.4 percent of total variation.

### 5.3 Confusion Matrix

The output of the computing done via all the classification algorithms is mapped via the confusion matrix. A confusion matrix consist of information about actual and predicted classes done by a classification system. Performance of such systems is evaluated using the data in the matrix. The following table shows the confusion matrix for a two class classifier. Confusion Matrix helps in detecting the accuracy of datasets.The data in the confusion matrix shown has the following meaning in context.

- a is the number of correct predictions that an instance is negative,
- b is the number of incorrect predictions that an instance is positive,
- c is the number of incorrect of predictions that an instance negative, and
- d is the number of correct predictions that an instance is positive.

**Table 5.1 Description of confusion matrix**

| | | Predicted | |
|---|---|---|---|
| | | Negative | Positive |
| Actual | Negative | **a** | **b** |
| | Positive | c | d |

### *5.4 Visualization of Results*

This section visualizes the results of the simulation carried out for the process of classification and detection of the brain tumour using MRI images with help of proposed methodology. The results express the design of graphical user interface with the help of the proposed methodology as well as the comparative analysis of the result with the help of comparison with the literature review. The comparison has also been done on the basis of analysis on various kernels based on SVM.

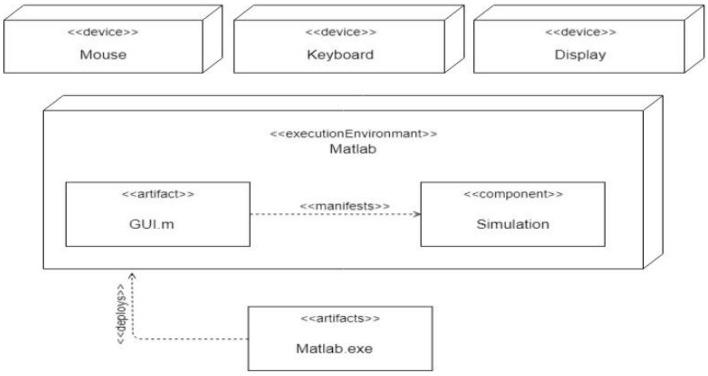

Figure 5.1 Deployment of methodology

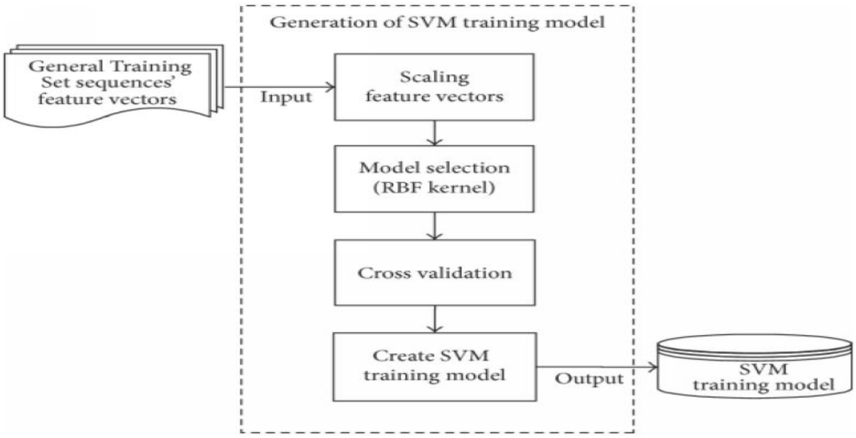

Figure 5.2 Description of kernel variation in improved SVM

Figure 5.3 Input image for sample class-1 (malignant)

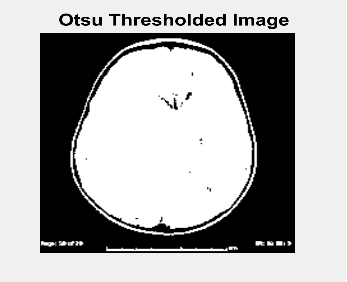

Figure 5.4 Otsu threshold image for malignant

**Figure 5.5 Cluster object for malignant**

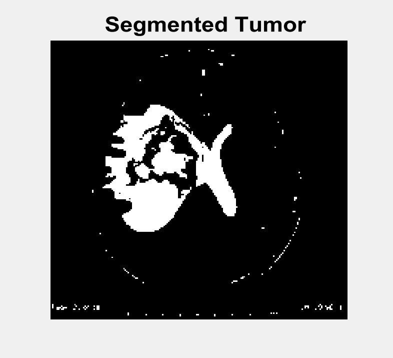

**Figure 5.6 Segmented tumor for malignant class**

Figure 5.3 to Figure 5.6 indicates the step by step segmentation output for sample of malignant tumour class. It was observed after analysis of simulation with various algorithms that the accuracy of linear kernel was 74% whereas accuracy of RBF kernel was 68% and Accuracy of polynomial kernel was 61.3333%.

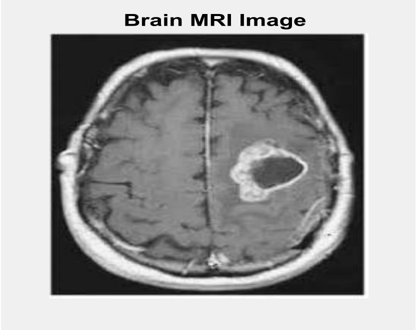

**Figure 5.7 Input Image for Sample Class-1 (benign)**

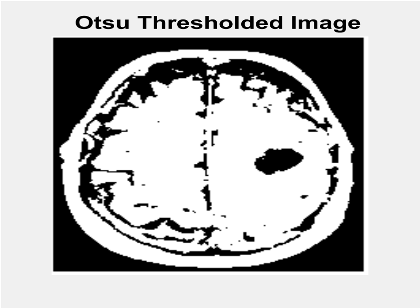

**Figure 5.8 Otsu threshold image for benign**

**Figure 5.9 Cluster object for benign**

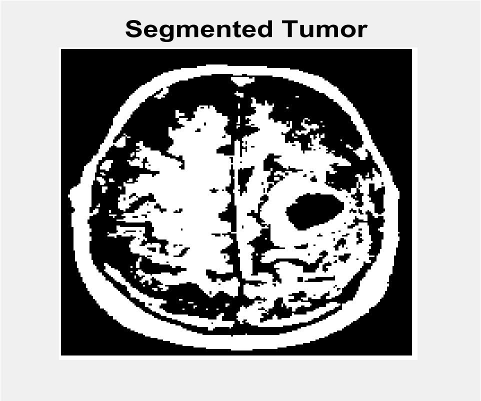

**Figure 5.10 Segmented tumor for benign class**

Figure 5.7 to Figure 5.10 indicates the step by step segmentation output for sample of benign tumour class. It was observed after analysis of simulation with various algorithms that the accuracy of linear kernel was 71 % whereas accuracy of RBF kernel was 58% and Accuracy of polynomial kernel was 56.43%.

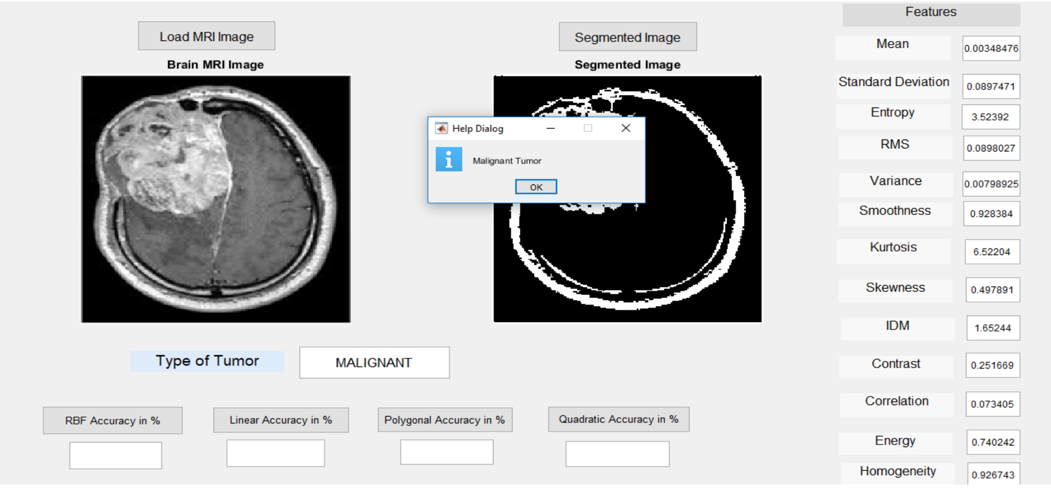

Malignant Tumor

Type of Tumor: MALIGNANT

| Features | |
|---|---|
| Mean | 0.00348476 |
| Standard Deviation | 0.0897471 |
| Entropy | 3.52392 |
| RMS | 0.0898027 |
| Variance | 0.00798925 |
| Smoothness | 0.928384 |
| Kurtosis | 6.52204 |
| Skewness | 0.497891 |
| IDM | 1.65244 |
| Contrast | 0.251669 |
| Correlation | 0.073405 |
| Energy | 0.740242 |
| Homogeneity | 0.926743 |

**Figure 5.11 GUI for detection of class-1**

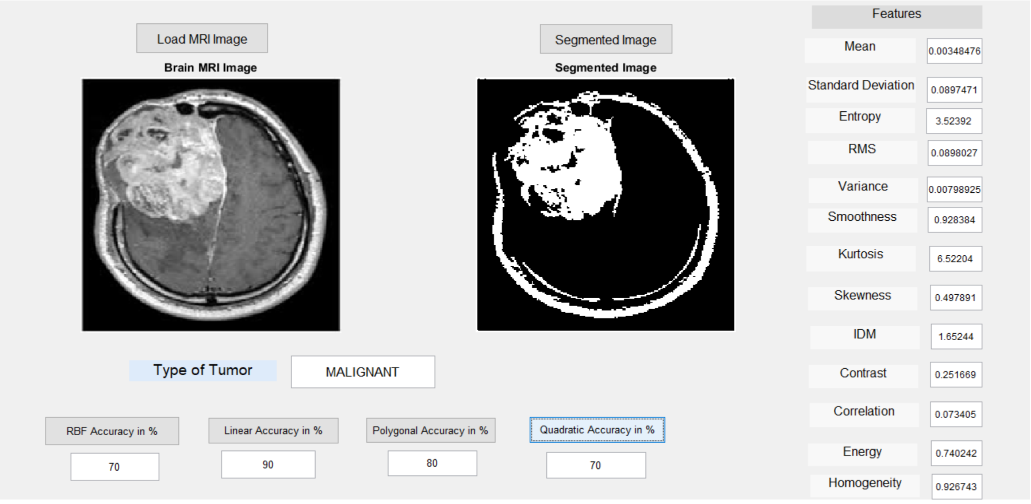

Type of Tumor: MALIGNANT

| Features | |
|---|---|
| Mean | 0.00348476 |
| Standard Deviation | 0.0897471 |
| Entropy | 3.52392 |
| RMS | 0.0898027 |
| Variance | 0.00798925 |
| Smoothness | 0.928384 |
| Kurtosis | 6.52204 |
| Skewness | 0.497891 |
| IDM | 1.65244 |
| Contrast | 0.251669 |
| Correlation | 0.073405 |
| Energy | 0.740242 |
| Homogeneity | 0.926743 |

| RBF Accuracy in % | Linear Accuracy in % | Polygonal Accuracy in % | Quadratic Accuracy in % |
|---|---|---|---|
| 70 | 90 | 80 | 70 |

Figure 5.12 Comparative analysis of accuracy class-1

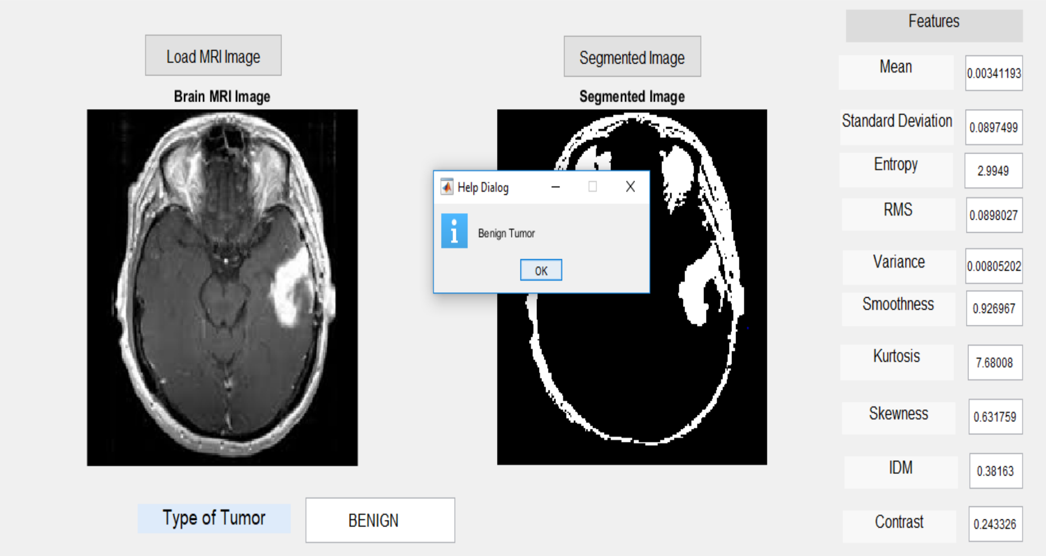

Benign Tumor

Type of Tumor: BENIGN

| Features | |
|---|---|
| Mean | 0.00341193 |
| Standard Deviation | 0.0897499 |
| Entropy | 2.9949 |
| RMS | 0.0898027 |
| Variance | 0.00805202 |
| Smoothness | 0.926967 |
| Kurtosis | 7.68008 |
| Skewness | 0.631759 |
| IDM | 0.38163 |
| Contrast | 0.243326 |

Figure 5.13 GUI for detection of class-2

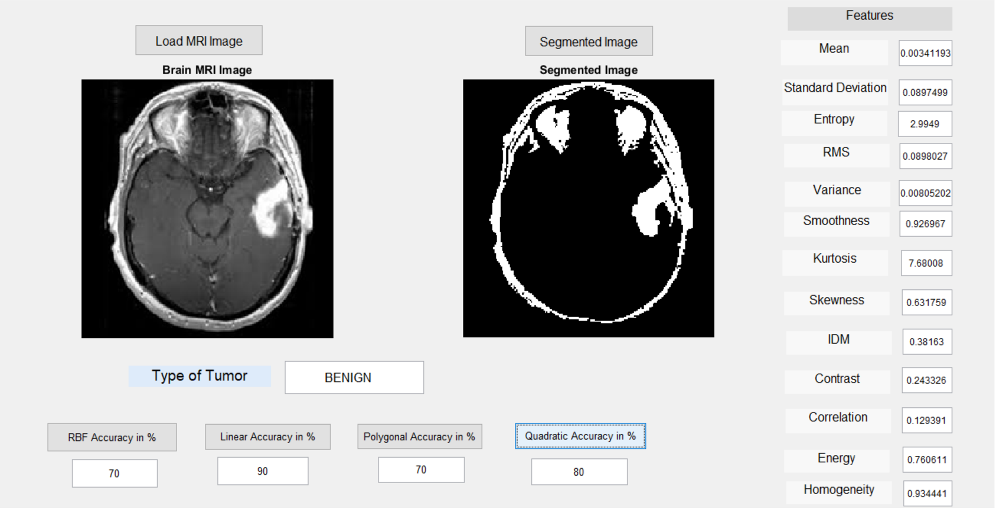

Type of Tumor: BENIGN

| Features | |
|---|---|
| Mean | 0.00341193 |
| Standard Deviation | 0.0897499 |
| Entropy | 2.9949 |
| RMS | 0.0898027 |
| Variance | 0.00805202 |
| Smoothness | 0.926967 |
| Kurtosis | 7.68008 |
| Skewness | 0.631759 |
| IDM | 0.38163 |
| Contrast | 0.243326 |
| Correlation | 0.129391 |
| Energy | 0.760611 |
| Homogeneity | 0.934441 |

| RBF Accuracy in % | Linear Accuracy in % | Polygonal Accuracy in % | Quadratic Accuracy in % |
|---|---|---|---|
| 70 | 90 | 70 | 80 |

Figure 5.14 Comparative accuracy analysis class-2

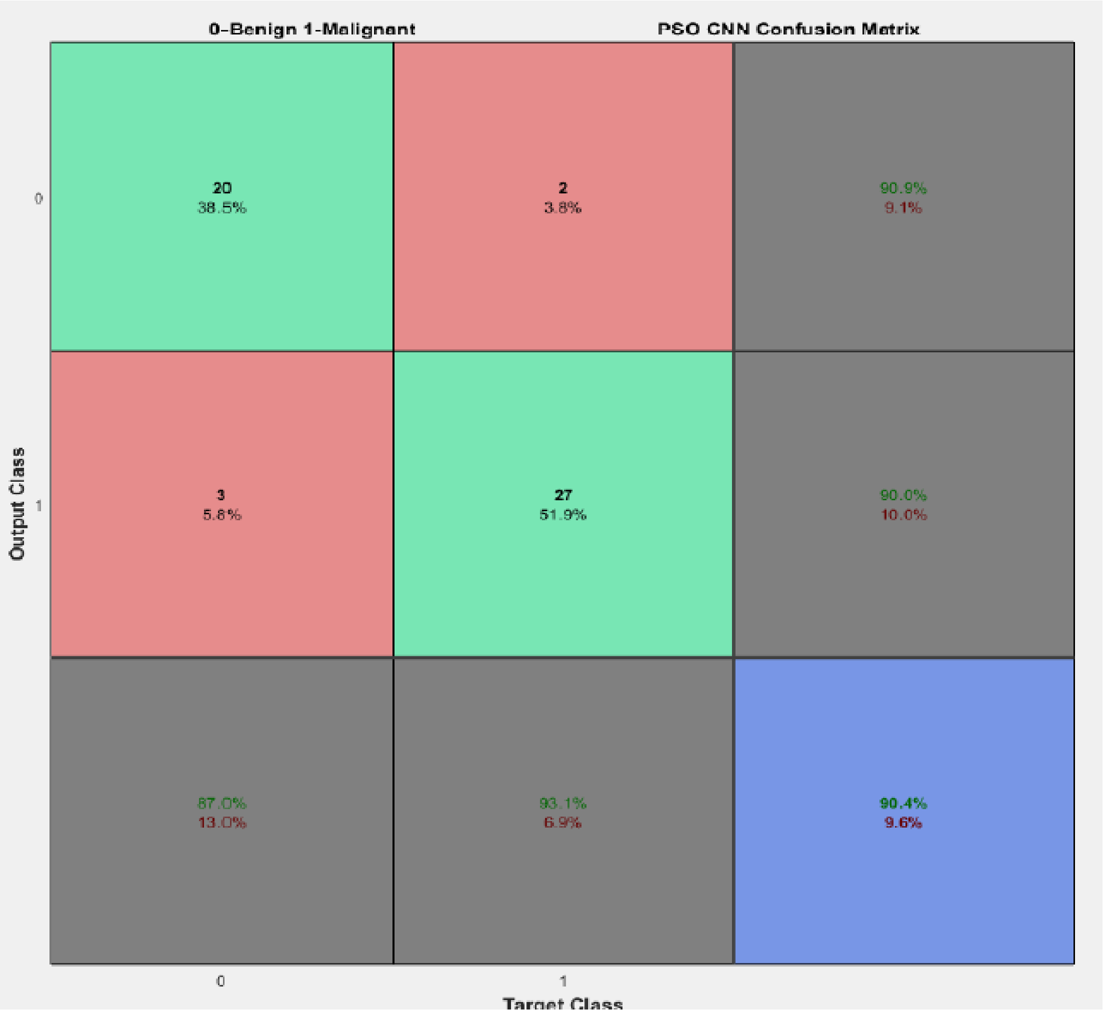

**Figure 5.15 Confusion Matrix for Proposed Methodology**

We put four SVMs to the test, each with a different kernel (LIN, HPOL, IPOL, and GRB). When a linear kernel is used, the KSVM degrades to the original linear SVM. Hundreds of simulations were run to determine the appropriate kernel function parameters, such as the order d in HPOL and IPOL kernels and the scaling factor ° in the GRB kernel. Table 5.2 shows the confusion matrices for our methods. After the supervised classification, the element of the ith row and jth column denotes the classification accuracy pertaining to class I is assigned to class j. The findings revealed that the suggested DWT+PCA+KSVM approach performs admirably on both training and validation images.

**Table 5.2**

**Confusion matrix of our DWT+PCA+KSVM method**

| | **LIN** | **Normal (O)** | **Abnormal (O)** |
|---|---|---|---|
| 1 | Normal (T) | 17 | 3 |
| | Abnormal (T) | 5 | 135 |
| 2 | **HPOL** | **Normal (O)** | **Abnormal (O)** |

| | | | |
|---|---|---|---|
| | Normal (T) | 19 | 1 |
| | Abnormal (T) | 4 | 136 |
| 3 | **IPOL** | **Normal (O)** | **Abnormal (O)** |
| | Normal (T) | 18 | 2 |
| | Abnormal (T) | 1 | 139 |
| 4 | **GRB** | **Normal (O)** | **Abnormal (O)** |
| | Normal (T) | 20 | 0 |
| | Abnormal (T) | 1 | 139 |
| (O denotes for output, T denotes for Target) | | | |

**Table 5.3Comparative analysis of accuracy**

| Approach from Literatures | Classification Accuracy (%) |
|---|---|
| DWT+SOM | 94 |
| DWT+SVM with linear kernel | 96 |
| DWT+SVM with RBF based kernel | 98 |
| DWT+PCA+ANN | 97 |
| DWT+PCA+kNN | 98 |
| DWT+PCA+ACPSO+FNN | 98.75 |
| **Approach from this work** | **Classification Accuracy (%)** |
| DWT+PCA+KSVM (LIN) | 95% |
| DWT+PCA+KSVM (HPOL) | 96.88% |
| DWT+PCA+KSVM (IPOL) | 98.12% |

HPOL kernel classification accuracy was (19+136)/160=97 percent; IPOL kernel classification accuracy was (18+139)/160 = 98 percent; and GRB kernel classification accuracy was (20+139)/ 160= 99 percent. The GRB kernel SVM, unsurprisingly, outperformed the other three kernel SVMs. Furthermore, we compared our method to six common methods (DWT+SOM, DWT+SVM with linear kernel, DWT + SVM with RBF based kernel, DWT+ PCA+ANN, DWT+PCA+k, DWT+PCA+KSVM with IPOL kernel, DWT+PCA+k, DWT+PCA+KSVM with IPOL kernel, DWT+PCA+k, DWT+PCA+ The average number represented the amount of time spent on each step. The average calculation time for feature extraction, feature reduction, and SVM classification for each 256256 image is 0.023 seconds, 0.0187 seconds, and 0.0031 seconds, respectively. The feature extraction stage takes the longest, taking 0.023 seconds. It takes 0.0187 seconds to reduce a feature. The SVM classification takes the shortest amount of time, only 0.0031 seconds. Each 256 X 256 pixel image takes roughly 0.0448 seconds to compute, which is fast enough for real-time diagnosis.

## 6. CONCLUSION AND FUTURE WORK

### *6.1 Conclusion*

Abnormal growth of tissue in the brain which affect the normal functioning of the brain is considered a brain tumor. The main goal of medical image processing is to identify accurate and meaningful information using algorithms with minimum error possible. Brain tumor detection and classification through MRI images can be categorized into four different sections: pre-processing, image segmentation, feature extraction and image classification. Various segmentation methodologies are explored in the work. It can be concluded that the algorithms and the parameters used in the proposed system are all meant to increase the efficiency of the system by achieving better results. The boundary approach and the edge based approach for segmentation are very common but the region growing approach gives better results. It is found that the particle swarm optimization algorithm gives the most accurately segmented tumors. Features extracted by using GLCM method help to increase efficiency as minute details of tumor by using various features can be extracted. Of the various classification methods studied, it was experimentally found that the convolution neural networks give the best classification accuracy. Accuracy and reliability are of utmost importance in tumor diagnosis, as a patient’s life depends on the results predicted by the system. Thus, the proposed methodology helps in increasing the accuracy and obtaining the desired results. We created a new DWT+PCA+KSVM approach to discriminate between normal and pathological brain MRIs in this work. We chose LIN, HPOL, IPOL, and GRB as four distinct kernels. The results show that the GRB kernel SVM has a classification accuracy of 99.38 percent on the 160 MR pictures, which is greater than HPOL, IPOL, and GRB kernels, as well as other popular approaches in recent literatures. The following four factors should be the focus of future work: To begin, the suggested SVM-based method might be used to process MR images with different contrast mechanisms, such as T1-weighted, Proton Density weighted, and diffusion weighted images. Second, advanced wavelet transforms such as the lift-up wavelet could be used to reduce calculation time. Third, multi-classification can be investigated, which focuses on specific illnesses evaluated using brain MRI. Finally, novel kernels will be evaluated in order to improve classification accuracy. The DWT extracts information from original MR images fast and with minimal loss. The spatial resolution of DWT over Fourier Transforms is an advantage, as it captures both frequency and location information. Although there are other excellent wavelets, such as the Daubechies series, we chose the Harr wavelet for this investigation. In future work, we will compare the performance of different wavelet families. The stationary wavelet transform and the wavelet packet transform are two further study areas.

### *6.2 Future Work*

Engineers constantly work on software for tumour detection and medical images processing. The segmentation of medical images is an important method for identifying tumours sometimes. This method is developed and supplemented by many scientists and researchers. In this project, the brain tumours of MRI images are identified using a GUI interface in Matlab. This software uses the Interface to produce the best performance using different segmentation combinations, filters and other image processing algorithms. In order to improve the accuracy of the proposed scheme, hybrid approaches may also be implemented

- Classification scheme of adaptive neuro fuzzy inference.
- Inclusion of the profound classification system learning system.
- Classification framework in real-time growth.
- Inclusion of Internet of things for improved applications and a real-time hardware interface system.

## REFERENCES

[1] Janvier, L., Olivier, P., Blonski, M., Morel, O., Vignaud, J.M., Karcher, G., Taillandier, L. and Verger, A., 2015. Correlation of SUV-derived indices with tumoral aggressiveness of gliomas in static 18F-FDOPA PET: use in clinical practice. Clinical nuclear medicine, 40(9), pp.e429-e435.

[2] Manisha Bhagwatl, R.K.Krishna&V.E.Pise, "Image Segmentation by Improved Watershed Transformation in Programming Environment MATLAB" ”international Journal of Computer Science & Communication Vol. 1, No. 2, pp. 171-174, 2010.

[3] M.H. FazelZarandia, M. Zarinbala, M. Izadi, "Systematic image processing for diagnosing brain tumors: A Type-II fuzzy expert system approach," ”plied soft computing, pp: 285-294, 2011

[4] Sandrasegaran, Kumaresan, Chandru P. Sundaram, Raja Ramaswamy, Fatih M. Akisik, Magnus P. Rydberg, Chen Lin, and Alex M. Aisen. "Usefulness of diffusion-weighted imaging in the evaluation of renal masses." American Journal of Roentgenology 194, no. 2 (2010): 438-445.

[5] Moorthy, Kohbalan, Aws Naser Jaber, MohdArfian Ismail, FerdaErnawan, MohdSaberi Mohamad, and SafaaiDeris. "Missing-values imputation algorithms for microarray gene expression data." Microarray Bioinformatics (2019): 255-266.

[6] Moorthy, Kohbalan, Aws Naser Jaber, MohdArfian Ismail, FerdaErnawan, MohdSaberi Mohamad, and SafaaiDeris. "Missing-values imputation algorithms for microarray gene expression data." Microarray Bioinformatics (2019): 255-266.

[7] M. Masroor Ahmed &Dzulkifli Bin Mohammad, "Segmentation of Brain MR Images for Tumor Extraction by Combining K-means Clustering and Perona-Malik Anisotropic Diffusion Model" ”international Journal of Image Processing, Vol. 2, No. 1, 2010

[8] Tse-Wei Chen, Yi-Ling Chen, Shao-Yi Chien, "Fast Image Segmentation Based on K-Means Clustering with Histograms in HSV Color Space" ”journal of Scientific Research, Vol. 44 No.2, pp.337-351, 2010.

[9] Pang, Yan-Mei, Qi Shan, Fu-Jun Zhou, Jie Hua, and Wen-Bin Hou. "Chemical constituents and pharmacological effects of genus Engelhardia." Chinese Herbal Medicines 10, no. 1 (2018): 2-13.

[10] Guo, Wen Lan, Zhi Jia Huang, and Yun Zhang. "The Application of Medical Robotics in the MRI-Guided Invention." In Advanced Materials Research, vol. 981, pp. 538-541. Trans Tech Publications Ltd, 2014.

[11] Dhingra, Naina, AmitaNandal, MeenuManchanda, and Deepak Gambhir … "Digital image watermarking using 2-DCT and 2-DWT in gray images." In 2017 InternationalConference on Intelligent Computing and Control Systems (ICICCS), pp. 797-803 68,

[12] Ghosal, Palash, Lokesh Nandanwar, Swati Kanchan, Ashok Bhadra, Jayasree Chakraborty, and Debashis Nandi. "Brain tumor classification using ResNet-101 based squeeze and excitation deep neural network." In 2019

Second International Conference on Advanced Computational and Communication Paradigms (ICACCP), pp. 1-6. IEEE, 2019..

[13] Suwalka, Isha, and Navneet Agrawal. "An improved unsupervised mapping technique using AMSOM for neurodegenerative disease detection." International Journal of Computational Systems Engineering 4, no. 2-3 (2018): 185-194.

[14] Saraswathi, D., B. Lakshmi Priya, and R. Punitha Lakshmi. "Brain tumor segmentation and classification using self organizing map." In 2019 IEEE international conference on system, computation, automation and networking (ICSCAN), pp. 1-5. IEEE, 2019.

[15] Mapari, Rakshanda M., and H. G. Virani. "Automated technique for segmentation of brain tumor in MR Images." In 2019 3rd International Conference on Trends in Electronics and Informatics (ICOEI), pp. 867-870. IEEE, 2019.

[16] Madhupriya, G., Narayanan M. Guru, S. Praveen, and B. Nivetha. "Brain tumor segmentation with deep learning technique." In 2019 3rd International Conference on Trends in Electronics and Informatics (ICOEI), pp. 758-763. IEEE, 2019.

[17] Zhang, Yandi, Xin Wang, Xiaoyi Bai, Ping Li, Di Su, Wen Zhang, Wei Zhang, and Bo Tang. "Highly specific Cys fluorescence probe for living mouse brain imaging via evading reaction with other biothiols." Analytical chemistry 91, no. 13 (2019): 8591-8594.

[18] C.J. Veenman, M.J.T. Reinders, E. Backer, “A maximum variance cluster algorithm”, IEEE Transactions on Pattern Analysis and Machine Intelligence, Vol. 24, No. 9, pp. 1273-1280, 2002.

[19] Alan Jose, S. Ravi, M. Sambath, “Brain tumor Segmentation using k-means clustering and Fuzzy c-means clustering And Its Area estimation”, International Journal of Innovation Research in Computer and Communication Engineering (IJIRCCE), Vol. 2, No. 3, 2014.

[20] Ansari, Irshad Ahmad, Millie Pant, Chang WookAhn, and JaehunJeong. "PSO optimized multipurpose image watermarking using SVD and chaotic sequence." In Bio-inspired computing-theories and applications, pp. 1-17. Springer, Berlin, Heidelberg, 2015.

[21] Dong, A. and Zeng, R., 2017, April. Research and Implementation Based on Three-Dimensional Model Watermarking Algorithm. In 2017 International Conference on Computing Intelligence and Information System (CIIS) (pp. 277-282). IEEE.

[22] Boykov, Yuri, and Vladimir Kolmogorov. "An experimental comparison of min-cut/max-flow algorithms for energy minimization in vision." IEEE transactions on pattern analysis and machine intelligence 26, no. 9 (2004): 1124-1137.

[23] Corso, Jason J., Eitan Sharon, Shishir Dube, Suzie El-Saden, Usha Sinha, and Alan Yuille. "Efficient multilevel brain tumor segmentation with integrated bayesian model classification." IEEE transactions on medical imaging 27, no. 5 (2008): 629-640.

[24] Fletcher-Heath, Lynn M., Lawrence O. Hall, Dmitry B. Goldgof, and F. Reed Murtagh. "Automatic segmentation of non-enhancing brain tumors in magnetic resonance images." Artificial intelligence in medicine 21, no. 1-3 (2001): 43-63.

[25] Kaus, Michael R., Simon K. Warfield, Arya Nabavi, Peter M. Black, Ferenc A. Jolesz, and Ron Kikinis. "Automated segmentation of MR images of brain tumors." Radiology 218, no. 2 (2001): 586-591.

[26] Khotanlou, Hassan, Olivier Colliot, and Isabelle Bloch. "Automatic brain tumor segmentation using symmetry analysis and deformable models." In Advances in Pattern Recognition, pp. 198-202. 2007.

[27] Diaz, Idanis, Pierre Boulanger, Russell Greiner, Bret Hoehn, Lindsay Rowe, and Albert Murtha. "An automatic brain tumor segmentation tool." In 2013 35th Annual International Conference of the IEEE Engineering in Medicine and Biology Society (EMBC), pp. 3339-3342. IEEE, 2013.

[28] Vanathe, V., S. Boopathy, and M. A. Manikandan. "MR image denoising and enhancing using multiresolution image decomposition technique." In 2013 International Conference on Signal Processing, Image Processing & Pattern Recognition, pp. 29-33. IEEE, 2013.

[29] Law, A. K. W., Hui Zhu, B. C. B. Chan, P. P. Iu, F. K. Lam, and F. H. Y. Chan. "Semi-automatic tumor boundary detection in MR image sequences." In Proceedings of 2001 International Symposium on Intelligent Multimedia, Video and Speech Processing. ISIMP 2001 (IEEE Cat. No. 01EX489), pp. 28-31. IEEE, 2001.

[30] Lin, Pan, Yong Yang, Chong-Xun Zheng, and Jian-Wen Gu. "An efficient automatic framework for segmentation of MRI brain image." In The Fourth International Conference on Computer and Information Technology, 2004. CIT'04., pp. 896-900. IEEE, 2004.

[31] Kouhi, Abolfazl, HadiSeyedarabi, and Ali Aghagolzadeh. "A modified FCM algorithm for MRI brain image segmentation." In 2011 7th Iranian Conference on Machine Vision and Image Processing, pp. 1-5. IEEE, 2011.

[32] Rajini, N. Hema, and R. Bhavani. "Enhancing k-means and kernelized fuzzy c-means clustering with cluster center initialization in segmenting MRI brain images." In 2011 3rd International Conference on Electronics Computer Technology, vol. 2, pp. 259-263. IEEE, 2011.

[33] Deepa, S. N., and B. Aruna Devi. "Artificial neural networks design for classification of brain tumour." In 2012 International Conference on Computer Communication and Informatics, pp. 1-6. IEEE, 2012.

[34] Kikuchi, Takuo. "Characteristic extraction from an ambiguous image using fuzzy mathematical morphology with adaptive structuring elements." In 10th IEEE International Conference on Fuzzy Systems.(Cat. No. 01CH37297), vol. 1, pp. 228-231. IEEE, 2001.

[35] Balafar, Mohd Ali, Abdul Rahman Ramli, M. Iqbal Saripan, and SyamsiahMashohor. "Review of brain MRI image segmentation methods." Artificial Intelligence Review 33, no. 3 (2010): 261-274.

[36] Manjón, José V., José Carbonell-Caballero, Juan J. Lull, Gracián García-Martí, Luís Martí-Bonmatí, and Montserrat Robles. "MRI denoising using non-local means." Medical image analysis 12, no. 4 (2008): 514-523.

[37] Bhandari, A., Koppen, J. &Agzarian, M (2020) Convolutional neural networks for brain tumour segmentation. Insights Imaging **11,** 77. https://doi.org/10.1186/s13244-020-00869-4.

[38] Jin KH, McCann MT, Froustey E, Unser M (2017) Deep convolutional neural network for inverse problems in imaging. IEEE Trans Image Process 26: 4509–4522.

[39] Yamashita R, Nishio M, Do RKG, Togashi K (2018) Convolutional neural networks: an overview and application in radiology. Insights Imaging 9:611–629.olving Nat., 2000, pp. 849–858.

[40] Dogiwal, Sanwta Ram, Y. S. Shishodia, Abhay Upadhyaya, Hanuman Ram, and Satish Kumar Alaria. "Image Preprocessing Methods in Image Recognition." *International Journal of Computers and Distributed Systems* 1, no. 3 (2012): 96-99.

[41] Koul, Deepali, and Satish Kumar Alaria. "A new palm print recognition approach by using PCA & Gabor filter." *International Journal on Future Revolution in Computer Science & Communication Engineering* 4.4 (2018): 38-45.

[42] Devender Kumar Dhaked, Yogender Kumar Sharma, Suman Bhakar (2021) “Highly Secured Digital Image Watermarking Using LSB and DCT,Combined Approach”, DE, pp. 1347 - 1356, Jun. 2021.

[43] Manish Kumar, Dr. Sunil Kumar, Dr. Harish Nagar, “Digital Image encryption based on Genetic Algorithm”, in *TEQIP-III Sponsored International Conference on Recent Trends in Engineering & Technology,* March 12-13, 2021 Organized by RTU, Kota & ACERC, Jaipur, ISBN No- 97893-5457-2630.

[44] Manish Kumar, Dr. Sunil Kumar, Dr. Harish Nagar, “Enhanced Text and Image Security using combination of DCT steganography, XOR Embedding and Arnold transform”, Journal of Design Engineering, pp. 732-739,Vol.2021, Issue 3, ISSN: 0011-9342.

[45] Manish Kumar, Dr. Sunil Kumar, Dr. Harish Nagar, “Enhanced Text Data and Image Security Using DCT Technique and Genetic Algorithm”, International Journal of TEST engineering and management, Vol.83, pp. 30566-30571, June 2020, ISSN: 0193-4120.